A NEW NUMERICAL MODEL OF THERMAL APERTURE CHANGES IN AN ENHANCED GEOTHERMAL SYSTEM RESERVOIR

Musa D Aliyu[1], Rosalind A Archer[1]

[1]Department of Engineering Science, the University of Auckland, Private Bag 92019, Auckland 1142, New Zealand.

musa.aliyu@auckland.ac.nz

r.archer@auckland.ac.nz

Keywords: *Thermal aperture, hydro-mechanical aperture, combined aperture, EGS reservoir, THM simulation.*

ABSTRACT

Extraction of energy from deep crystalline formation requires pressurisation of the rock mass to create new or enhance existing natural fractures. The fractures generate a pathway for transport of the fluid and heat back to the surface for optimum energy production. However, the complexity of fracture aperture opening and closure during exploitation has posed a challenge for both engineers and geologists. The most widely used model for fracture aperture changes is frequently limited to the hydro-mechanical effect only. This paper presents a new model that incorporates a complete cycle of thermal, hydraulic and mechanical aperture changes in an enhanced geothermal system (EGS) reservoir using a coupled thermo-hydro-mechanical (THM) simulator. The goal is to understand the extent to which thermal aperture changes might enhance the performance of EGS reservoirs. Three reservoir cases are developed: a model of hydro-mechanical aperture changes with a constant thermal aperture; a model of thermal aperture changes employing a constant hydro-mechanical aperture; and a combined model of both hydro-mechanical and thermal aperture changes. The outcomes show that the changes are greater with the thermal aperture than with the hydro-mechanical aperture due to the impact of thermal contraction.

1. INTRODUCTION

In hot dry rock (HDR) systems, fractures often control the transportation of fluid and heat because their permeability is usually larger than that of the surrounding rock masses. The permeability of fractures changes as they open or close from the resultant shift in effective stress, pore pressure, chemical equilibrium and temperature (Abé et al., 1985, 1979; Abé and Sekine, 1983). The effect of thermal, hydraulic, mechanical and chemical (THMC) processes on variations in fracture permeability must be observed in tangent with one another because they can work together to produce either a closure or opening of a fracture (Willis-Richards and Wallroth, 1995). For instance, in an enhanced geothermal system (EGS) reservoir, maintaining a fracture network of sufficiently high permeability is crucial to ensure the continuous exchange of heat between the rock matrix and the circulation fluid.

The application of coupled THMC processes via modelling or laboratory experiments might increase the chances of extracting heat from EGS reservoirs and improve their operations under economically viable conditions. It is crucial to investigate the effect of THMC processes in fractures by employing well-calibrated models for the accurate prediction of the long-term performance of EGS reservoirs. Considerable efforts have been made towards modelling the effects of hydraulic fracturing on EGS reservoirs using numerous coupled process-based techniques (Taron and Elsworth, 2010, 2009).

One of the earliest coupled thermo-hydro-mechanical (THM) models was developed by Harlow and Pracht (1972) using the finite difference (FD) method. They developed several conceptual models of HDR geothermal reservoirs to study the effect of hydraulic fracturing on thermal energy extraction. McFarland (1975) developed a two-dimensional (2D) FD model to represent the operation of an HDR geothermal reservoir with a penny-shaped crack created by hydraulic fracturing. Abé et al. (1976b) investigated the stable growth of a penny-shaped crack created by hydraulic fracturing in an HDR geothermal reservoir using a coupled THM solution. In another study, they examined the growth of a vertical penny-crack induced because of hydraulic fracturing operation during heat extraction from an HDR reservoir (Abé et al., 1976a).

Furthermore, Bažant and Ohtsubo (1978) employed McFarland's geometrical approach to developing a finite element (FE) model of an HDR geothermal reservoir using coupled THM processes to investigate the effect of temperature changes on crack thickness. DuTeaux et al. (1996) developed a fully coupled THM FE code called GEOCRACK to investigate the variations in the properties of rock joints during HDR geothermal exploitations. Kohl et al. (1995) studied the response of a fractured medium to hydraulic stimulation in an HDR system using a FRACTure coupled THM processes simulator. Hicks et al. (1996) employed HOTGRID code to model the potential coupled effects of THM processes in an HDR geothermal reservoir's heat extraction. Ghassemi et al. (2003) developed an integral equation to study the effect of induced thermal stress during an EGS reservoir extraction. Taron et al. (2009) proposed a coupled THMC framework by connecting TOUGHREACT and FLAC3D packages to analyse the physical interactions of deformable fractured porous media.

The above literature presents a few THMC models that have been developed to investigate the various aspect of hydraulic fracturing effects on EGS reservoirs. However, despite these efforts, a need still exists for a standard code to model thermal aperture changes in EGS reservoirs, particularly in three-dimensions (3D). Thus, this study presents a new approach to establishing the thermal aperture variation in 3D EGS reservoirs using a coupled THM simulation. The new model incorporates a complete cycle of thermal, hydraulic and mechanical aperture change effects in an EGS reservoir. The goal of this research is to understand the extent to which thermal aperture changes might enhance the performance of the system. Three reservoir cases were developed: a model of hydro-mechanical aperture changes with a constant thermal aperture, a model of thermal aperture changes employing a

constant hydro-mechanical aperture and a combined model using both hydro-mechanical and thermal aperture changes.

Within this study, the numerical approach is implemented in the COMSOL Multiphysics Solver to investigate the different aperture change models. The solver provides the means to modify the built-in partial differential equations (PDEs) and supports the implementation of different functions. The simulator is capable of handling coupled THM processes of EGS reservoirs (Aliyu and Archer, 2020a), as previously validated, against the experimental measurement of the Fenton Hill HDR geothermal field in New Mexico (Aliyu and Archer, 2020b, 2020c; Aliyu and Chen, 2018).

2. MATHEMATICAL FORMULATION

There are many studies that formulate the mathematical models describing the behaviour of coupled THM processes in EGS reservoirs. These equations were derived from the laws of energy conservation, momentum and mass using Fourier's law, Hooke's law and Darcy's law, respectively. Therefore, this study provides the fracture aperture models to avoid repetition.

2.1 Hydro-mechanical aperture model

Figure 1 displays a fracture aperture model subject to hydraulic (pressure, p) and mechanical (normal stress, σ_n) loading. High-pressure injection alters the stress regime and the normal stiffness, K_n, of the fracture that allows it to either open or close. The effective stress, σ_n', on the fracture can be expressed as

$$\sigma_n' = \sigma_n - \alpha p \quad (1),$$

where α is the Biot coefficient. The relationship between fracture aperture, b_{hm}, and the effective stress is given as

$$b_{hm} = b_0 - \frac{\sigma_n'}{K_n} \quad (2),$$

where b_0 is the initial fracture aperture at initial loading. Bandis et al. (1983) describe the fracture closure, ΔV_j, under increasing stress and relate it to effective stress, expressed as

$$\Delta V_j = \frac{\sigma_n'}{K_{ni} + \frac{\sigma_n'}{b_{\max}}} \quad (3),$$

where $b_{\max}$ is the maximum fracture closure and K_{ni} is the initial stiffness of the fracture. The normal stiffness, K_{ni}, is given as (Barton et al., 1985)

$$K_n = \frac{\partial \sigma_n'}{\partial \Delta V_j} = K_{ni}\left[1 - \frac{\sigma_n'}{b_{\max} K_{ni} + \sigma_n'}\right]^{-2} \quad (4).$$

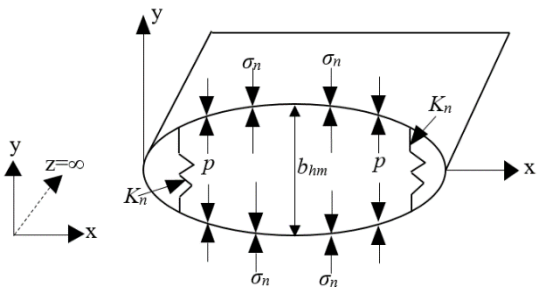

Figure 1: Fracture aperture subject to normal stress and pressure

2.2 Thermal aperture model

For the purposes of the thermal energy equation, the source term Q consists of heat conduction and energy convection by moving fluid along the fracture, which is expressed as (McFarland, 1975)

$$Q = \frac{1}{C_P}\left[\frac{2q}{b_T} - C_P \rho\left(\frac{dT}{dt}\right)\right] \quad (5),$$

where C_P is the heat capacity of the fluid, b_T is the thermal aperture, ρ is the fluid density, and q is the heat flux into the fracture surface from the surrounding rock on both sides of the fracture, given as

$$q = 2h(T_i - T) \quad (6).$$

Here, h is the effective heat transfer coefficient, T_i is the initial rock temperature and T is the temperature at any given time. The temperature gradient at a given time determines the rate of heat transfer from the rock into the fracture. The term h can be determined using several approaches. For example, the thermal diffusivity of granite ($10^{-6} m^2/s$) could be used to obtain the thermal penetration depth of cooling δ. Based on granite thermal diffusivity, McFarland (1975) proposed an approximate value of 100 m in 30 years. The heat transfer coefficient, h, and the thermal penetration depth, δ, are related through an analytical solution written as

$$h \approx \frac{4\lambda_r}{\delta} \quad (7),$$

where λ_r is the thermal conductivity of the rock. The thermal penetration depth of cooling is given as (Bažant and Ohtsubo, 1978)

$$\delta = \sqrt{\frac{12 t \lambda_r}{\rho_r C_r}} \quad (8),$$

where ρ_r is the density of the rock and C_r is the heat capacity of the rock. Equating expression (8) into (7) yields

$$h \approx \sqrt{\frac{\lambda_r \rho_r C_r}{3t}} \quad (9).$$

Proceedings 42nd New Zealand Geothermal Workshop
24-26 November 2020
Waitangi, New Zealand
ISSN 2703-4275

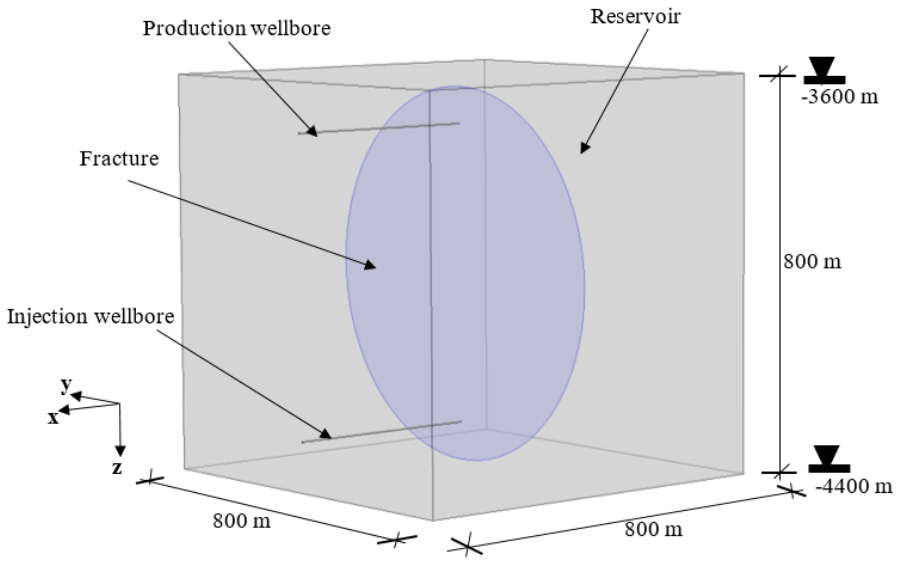

Figure 2: Reservoir geometry

To calculate the thermal aperture, b_T, of the fracture, the two primary contributors to the opening of the fracture are the thermal penetration depth of cooling and the thermal contraction of the rock due to cooling. By assuming a parabolic temperature profile in the rock, the thermal aperture opening is given as (Bažant and Ohtsubo, 1978)

$$b_T = \frac{2\alpha_r}{3(1-\upsilon)}(T_i - T)\delta \quad (10),$$

where α_r is the coefficient of free thermal dilation and υ is the Poisson's ratio of the rock. The sum of the hydro-mechanical aperture, b_{hm}, and the thermal aperture, b_T, within a vertically oriented penny-shaped fracture may be approximated as

$$b = b_{hm} + b_T \quad (11).$$

Equation (11) provides a rough estimate of the combined fracture aperture variation concerning the hydraulic (pressure), mechanical (effective stress and stiffness) and temperature (thermal contraction and penetration depth) processes.

3. MODEL DESCRIPTION

The Fenton Hill HDR project has provided a wide range of information for the development of EGS reservoir models for simulation studies (Dash et al., 1983; Murphy et al., 1981). In the context of this study, using the site data along with some reasonable assumptions based on other EGS sites, such as Soultz (France) (Aliyu, 2018; Aliyu and Chen, 2016; Aliyu and Chen, 2017) and Rosemanowes (UK) (Willis-Richards, 1995) were employed to set up a 3D numerical model. The model set up assumes that the reservoir is linearly elastic, homogenous and isotropic, and has a local thermal equilibrium between the rock and fluid and a fully saturated system (Aliyu et al., 2017, 2016).

3.1 Model configuration

Figure 2 presents the geometry of the EGS reservoir employed in this study. The dimensions of the reservoir are 800 m × 800 m × 800 m. The wellbores have a horizontal length of 400 m with the injection wellbore located at 400 m (y-axis) and -4,300 m (z-axis), and the production well is positioned at 400 m (y-coordinate) and -3,700 m (z-coordinate). The fracture has a radius of 375 m positioned at 400 m (x-axis) with a vertical centre of 4000 m.

Physical properties of the reservoir comprise: thermal conductivity (2.9 W/m/K), heat capacity (850 J/kg/K), density (2600 kg/m^3), Young's modulus (60 GPa), porosity (0.2), permeability (1e-18 m^2), Biot coefficient (0.79), Biot modulus (1.23e+4 MPa), coefficient of thermal expansion (7e-6 1/K) and solid bulk modulus (50 GPa). The fracture properties are: thermal conductivity (2.5 W/m/K), heat capacity (900 J/kg/K), density (2000 kg/m^3), Young's modulus (40 GPa), porosity (0.1), initial aperture (0.5 mm), maximum fracture closure (0.02 mm), initial fracture stiffness (1e+5 MPa/m).

For initial and boundary conditions, the initial pressure value employed for the hydraulic condition is hydrostatic. The authors employed 10 MPa injection pressures in order to replicate the joint opening pressure at the Fenton Hill Phase 1 reservoir, which is 10.3 MPa (surface value) (Kelkar et al., 2016). The initial temperature value used for the thermal condition depends on surface temperature, geothermal gradient and depth, given as,

$$T_{init} = 12°C - 0.04(K/m) \times z \quad (12),$$

The injection temperature employed is 40°C. For the geomechanical condition, the initial stress components for the vertical, maximum and minimum horizontal is given as

$$\sigma_{V_0} = 57\,(MPa) - \alpha_b \times p_0 \quad (13),$$

$$\sigma_{H_0} = 50\,(MPa) - \alpha_b \times p_0 \quad (14),$$

$$\sigma_{h_0} = 37\,(MPa) - \alpha_b \times p_0 \quad (15).$$

Proceedings 42nd New Zealand Geothermal Workshop
24-26 November 2020
Waitangi, New Zealand
ISSN 2703-4275

Roller boundary conditions are assigned on all sides except the top, where the vertical stress component of 57 MPa is applied. For the maximum horizontal stress, 50 MPa is employed at the front and back surfaces, and 37 MPa minimum horizontal stress is applied at the right and left boundaries.

The initial and boundary conditions are employed to investigate three scenarios of the fracture aperture models. The results of the simulations are displayed and examined in the following sections of the paper.

4. RESULTS AND DISCUSSION

This section presents the simulation results obtained from the three different aperture models. It analyses the temperature breakthrough curves, the effect of aperture changes at the injection location, the shear stresses, the fracture surface pressure changes, the thermal front growth on the fracture surface and the fracture aperture evolution on the surface.

4.1 Temperature breakthrough curves

Figure 3 displays the temperature breakthrough curves at the production point for the different aperture models. The outlet temperature for the thermal aperture models falls rapidly over time. After about 50 days for the combined hydro-mechanical and thermal aperture models, and 150 days, for the thermal aperture model, of circulation, it drops below a level that could be used for power generation. It is clear from the results that for a single fracture system, the thermal aperture model is not feasible for geothermal energy prediction. The decrease in the heat transfer rate from the hot rock causes a rapid drop in the outlet temperature (Aliyu and Chen, 2017). The correct process for making the thermal aperture model more feasible for a geothermal scheme is through adding the effect of multifracture system and secondary fracturing due to cooling.

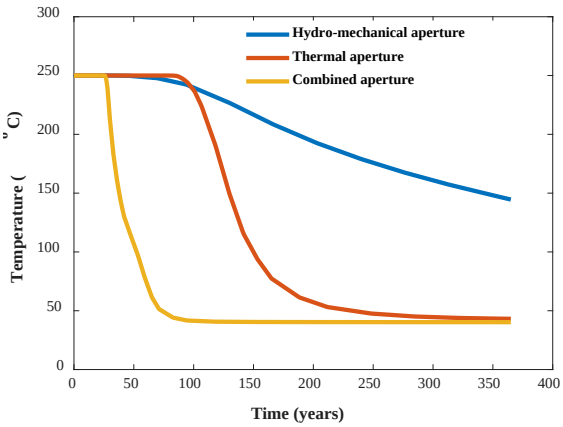

Figure 3: Fracture temperature at the production point for hydro-mechanical, thermal and combined aperture models

4.2 Aperture changes

Aperture change is monitored at injection locations for the different models, as shown in Figure 4. Each curve portrays the contribution of a different aperture model. The combined influence of hydro-mechanical and thermal aperture change refers to the contribution from all processes and so reflects the visible variation in reservoir permeability. The fracture opens with time in all the scenarios as cold fluid injection causes the system to thermally contract due to the dominance of fluid pressure, which increases the fracture aperture. The thermal aperture enlargement is more pronounced; it is more than 12 times the hydro-mechanical aperture changes. The reason for this behaviour is two-fold: the cold fluid injection causes the fracture to contract, which leads to a greater opening width of the aperture and a lower rate of heat transfer to the fracture due to a thermal front effect (Bažant et al., 1979).

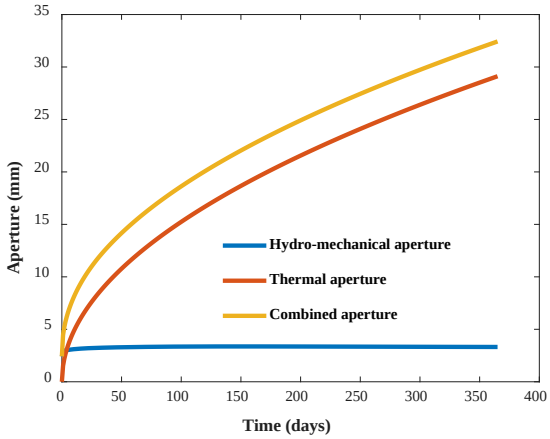

Figure 4: Fracture aperture changes at injection point for hydro-mechanical, thermal and combined models

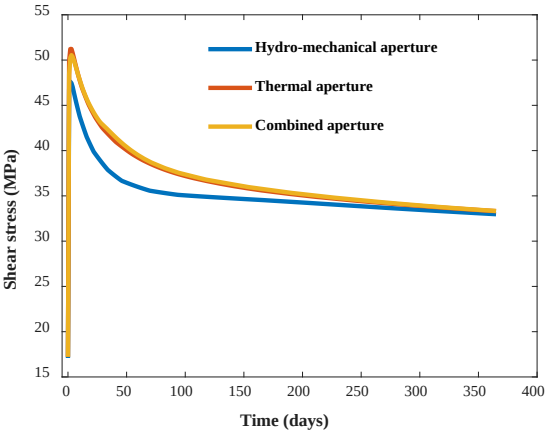

Figure 5: Fracture shear stress at the production point for hydro-mechanical, thermal and combined aperture models

4.3 Shear stress changes

Figure 5 shows the fracture shear stress curves at the production point for the different aperture models. During the first day of injection, the shear stress at the fracture built-up and increased rapidly until a maximum value of 51.5 MPa, 48 MPa, and 51 MPa were obtained for the thermal, hydro-mechanical and combined aperture models, respectively. The shear stress gradually decayed for the different models for the remainder of the simulation period. Creeping along the fracture plane could be the possible reason for the decay. The decrease in shear stress observed between day 50 and day 365 could be the result of the blockage at the edge of the fracture surface by the impermeable rock. It could have resulted in shear surface becoming the dominant failure plane. Had the simulation been run with multiple fracture systems, the fracture surface may have evolved into the dominant slip surface.

Proceedings 42nd New Zealand Geothermal Workshop
24-26 November 2020
Waitangi, New Zealand
ISSN 2703-4275

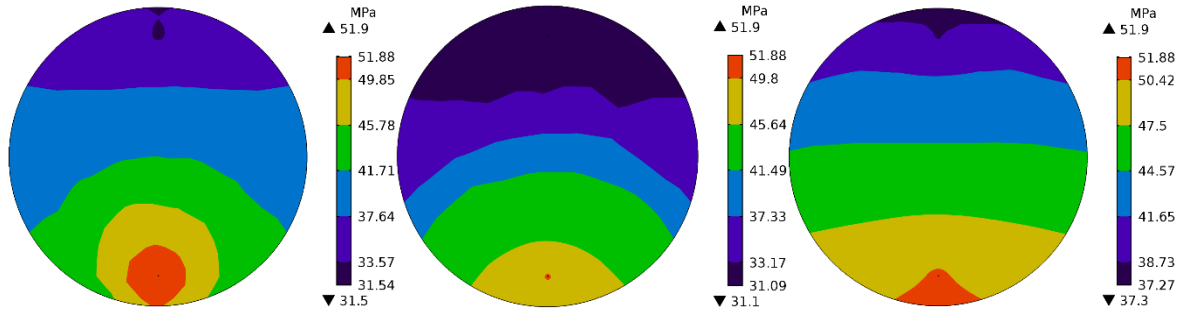

a. Pressure, $b_{hm,}$ (60 days) **b. Pressure, $b_{T,}$ (60 days)** **c. Pressure, $b_{hm}+b_{T,}$ (60 days)**

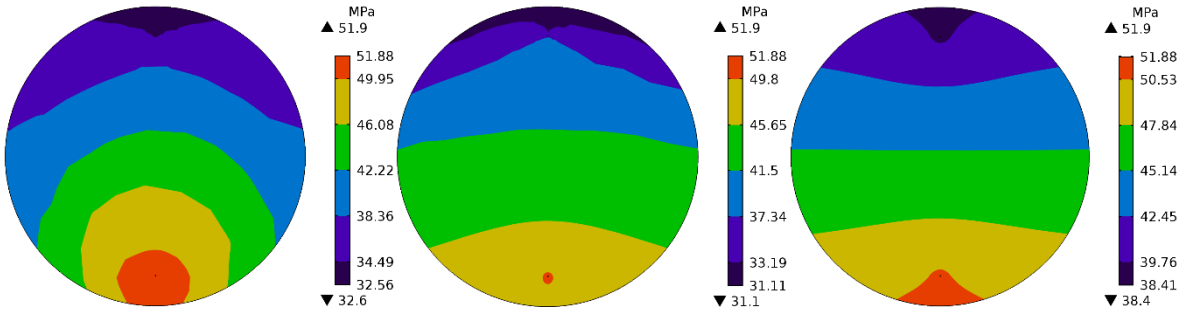

d. Pressure, $b_{hm,}$ (120 days) **e. Pressure, $b_{T,}$ (120 days)** **f. Pressure, $b_{hm}+b_{T,}$ (120 days)**

Figure 6: Fracture pressure evolution contours for hydro-mechanical (left), thermal (middle) and combined (right) aperture models at various simulation stages

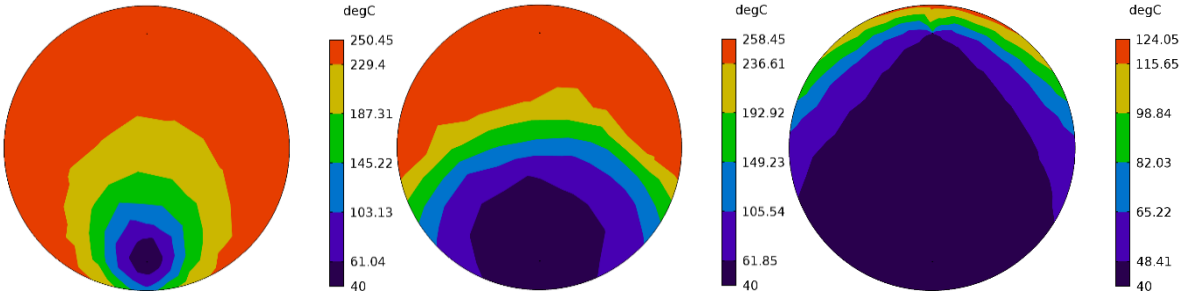

a. Thermal front, $b_{hm,}$ (60 days) **b. Thermal front, b_T (60 days)** **c. Thermal front, $b_{hm}+b_{T,}$ (60 days)**

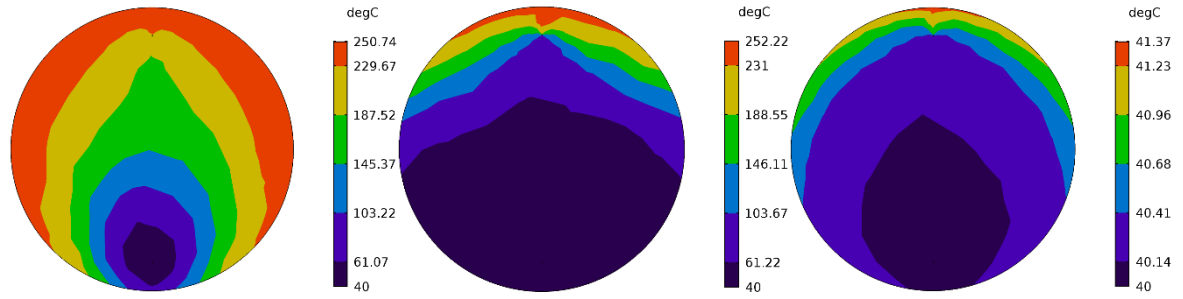

d. Thermal front, b_{hm} (120 days) **e. Thermal front, b_T (120 days)** **f. Thermal front, $b_{hm}+b_{T,}$ (120 days)**

Figures 7: Fracture thermal front evolution contours for hydro-mechanical (left), thermal (middle) and combined (right) aperture models at various simulation stages

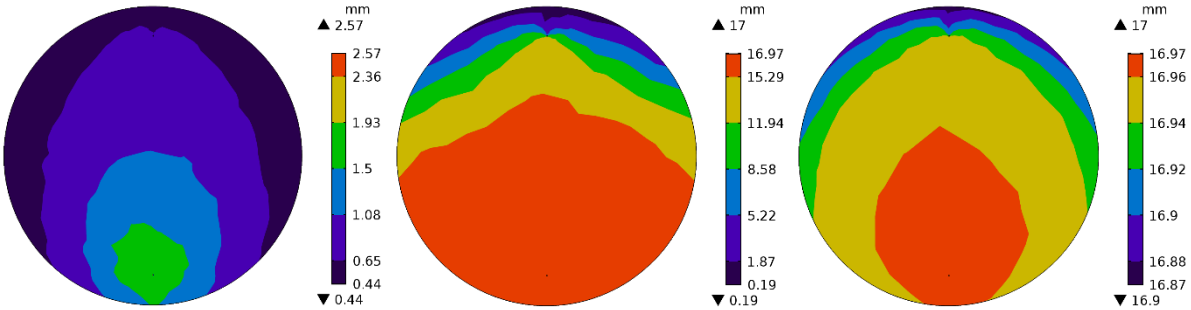

a. Hydro-mechanical aperture (124 days) **b. Thermal aperture (124 days)** **c. Combined model (124 days)**

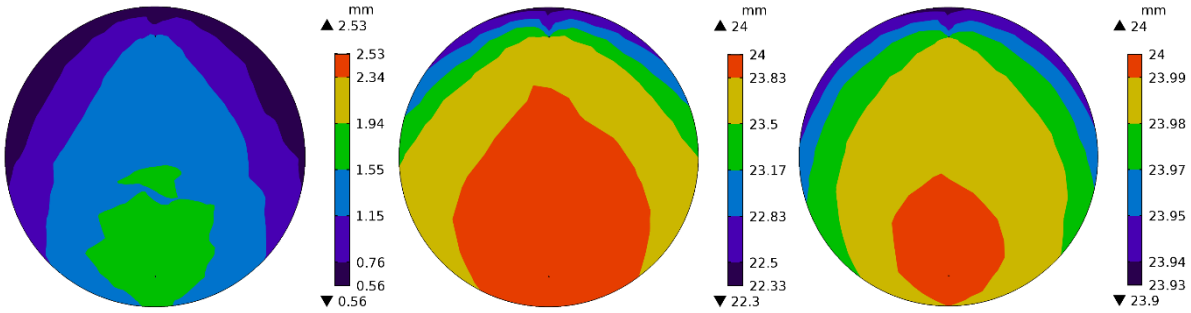

d. Hydro-mechanical aperture (248 days) **e. Thermal aperture (248 days)** **f. Combined model (248 days)**

Figure 8. Fracture aperture growth contours for hydro-mechanical (left), thermal (middle) and combined (right) aperture models at various simulation stages

4.4 Pressure evolution on fracture surface

Figure 6 presents the pressure fields on the surface of the fracture for the different aperture models. As can be seen, the pressure increases and strongly intensifies with the progressive cooling. The pressure increase is directed toward the top of the fracture where the production outlet is positioned. It shows that water molecules travel a longer path in the hot rock, which improves the effectiveness of heat extraction (Bažant and Ohtsubo, 1978). This phenomenon is promising for geothermal operations because it allows cooling to occur at the hottest points of the rock. The downward flow at the injection location is because of gravity and buoyancy since colder water is denser (Bažant and Ohtsubo, 1978).

The pressure losses in an open fracture are generally small so that injection rate depends on the pressure drop in the wellbores and at the surface plant. The pressure rises on the fracture surface due to the fluid density changes for the different aperture models being about 1.5 MPa at early stages and increasing as the production temperature decreases. In all the cases shown in Figure 6, the fractures begin to open by the same injection pressure, so that the pressure is different in each scenario. The expansion of a fracture by constant fluid flow injection is a typical problem of reservoir simulation (Abé et al., 1985). The results presented in this study are valid for a single planar fracture where the effects of pressure, temperature and stress changes on the rock are considered.

4.5 Thermal front growth on fracture surface

Figure 7 displays the thermal front growth on the surface of the fracture for the different aperture models. As seen, the thermal front is more pronounced in thermal aperture models (Figures 7b, 7c, 7e, and 7f) than the hydro-mechanical aperture model (Figures 7a, and 7d). The thermal aperture model considers the temperature variation as a primary parameter for its aperture changes in which the cold fluid injection impacted it the most. The wider opening of the fracture primarily causes the size of the thermal front to increase, as shown in Figuress—7e and 7f, respectively. The cold fluid cools the surface of the fracture near the injection location resulting in the fracture volume increasing from the thermal contraction of the hot rock. The surface area exposed to the cold fluid effect increases with time as a result of a significant temperature difference between the host rock and the fluid.

4.6 Aperture propagation on fracture surface

Figure 8 presents the fracture aperture propagation contours on the fracture surface for the different aperture models. The increasing magnitude of the temperature difference between the hot rock and the cold fluid intensifies the broader opening of the fracture at later times in cases of thermal aperture models. For the hydro-mechanical aperture model, however, the increase is less pronounced for the different time stages. The fracture opening becomes more pronounced with time, enhanced by the thermal contraction of the hot rock in the colder regions due to the thermal front effect as shown by the fracture aperture contours.

For the combined aperture model, the maximum fracture aperture has increased from an initial value of 2.5 mm to 16.97 mm after 124 days and moved up to the injection location, as shown in Figure 6c. In the case of thermal aperture, the aperture has increased from the initial 0 mm to 16.97 mm after 124 days, as indicated in Figure 8b. Whereas for the hydro-mechanical aperture model, the fracture aperture opening distributed the surface between 0.44 mm to 2.57 mm, as shown in Figure 6a. Similarly, these figures show

the pattern of fracture aperture growth in unequal increments of thickness from the lower opening at the outer boundary (fracture edges) to the maximum opening at the injection location.

The following general trends are observed in Figures 7 and 8: the steeper the thermal front of the fracture surface, the more significant the aperture opening is. This attribute is not favourable to the extraction of heat from HDR by the assumption of a single planar fracture undergoing cold fluid circulation. The early cooling of the fracture surface corresponds to pure heat convection because of cold fluid injection that causes a broader opening in the aperture. It leads to increased fluid flow in the cooling fracture, which consequentially yields a drop in the temperature contour with a steeper thermal front. Thus, this behaviour inhibits the further increase in the fracture aperture and therefore hinders the fluid circulation in the cooling fracture.

5. CONCLUSION

This paper has presented three numerical models of an EGS reservoir using coupled THM simulation processes to examine the effect of different aperture models on the system's performance. Three aperture models – hydro-mechanical, thermal, and combined thermo-hydro-mechanical – were implemented in the COMSOL Multiphysics solver for the investigation. Several reservoir parameters were analysed by comparing how each parameter responded to the different models.

The results show that the hydro-mechanical aperture model has less effect on EGS reservoir performance. In comparison, the thermal and the combined aperture models have the most pronounced effect out of all the parameters investigated. It is essential to point out that the thermal aperture model implementation is hard to find studies of in the existing literature due to its complexity, which makes this study unique in some ways. The model is highly non-linear; therefore, the results must be looked at with discretion and should not be assumed to be perfectly accurate.

The thermal aperture model results seem favourable for some aspects of an EGS energy extraction scheme. However, the model requires further study to answer some crucial questions. For example, how will heat convection in a secondary fracture affect the aperture opening of the primary fracture? Is it possible to create a pattern of the secondary fracture in a 3D model? How will the primary fracture extend or close with the addition of secondary fractures?

REFERENCES

Abé, H., Hayashi, K., Arima, S., 1985. Theoretical study on the stability of a reservoir created by the intersection of a fluid-filled crack with an oblique joint for the extraction of geothermal heat. Int. J. Numer. Anal. Methods Geomech. 9, 15–27.

Abé, H., Keer, L.M., Mura, T., 1976a. Growth rate of a penny-shaped crack in hydraulic fracturing of rocks, 2. J. Geophys. Res. 81, 6292–6298.

Abé, H., Keer, L.M., Mura, T., 1979. Theoretical study of hydraulically fractured penny-shaped cracks in hot, dry rocks. Int. J. Numer. Anal. Methods Geomech. 3, 79–96.

Abé, H., Mura, T., Keer, L.M., 1976b. Growth rate of a penny-shaped crack in hydraulic fracturing of rocks. J. Geophys. Res. 81, 5335–5340.

Abé, H., Sekine, H., 1983. Crack-Like Reservoir in Homogeneous and Inhomogeneous HDR. In: Springer. Springer, pp. 447–462.

Aliyu, M.D., 2018. Hot dry rock reservoir modelling. University of Greenwich.

Aliyu, M.D., Archer, R.A., 2020a. Numerical simulation of multifracture HDR geothermal reservoirs. Renew. Energy. Doi: 10.1016/j.renene.2020.09.085

Aliyu, M.D., Archer, R.A., 2020b. Thermo-hydro-mechanical model of multifracture HDR geothermal reservoirs. Geotherm. Resour. Counc. Trans. 44, 1–28.

Aliyu, M.D., Archer, R.A., 2020c. Numerical simulation of HDR geothermal energy reservoirs: A thermo-hydro-mechanical model. Geotherm. Resour. Counc. Trans. 44, 1–26.

Aliyu, M.D., Chen, H.-P., 2016. Numerical modelling of coupled hydro-thermal processes of the Soultz heterogeneous geothermal system. In: ECCOMAS Congress 2016 - Proceedings of the 7th European Congress on Computational Methods in Applied Sciences and Engineering.

Aliyu, Musa D., Chen, H.-P., 2017. Sensitivity analysis of deep geothermal reservoir: Effect of reservoir parameters on production temperature. Energy 129, 101–113.

Aliyu, M.D., Chen, H.-P., 2018. Enhanced geothermal system modelling with multiple pore media: Thermo-hydraulic coupled processes. Energy 165, 931–948.

Aliyu, Musa D, Chen, H., 2017. Optimum control parameters and long-term productivity of geothermal reservoirs using coupled thermo-hydraulic process modelling. Renew. Energy 112, 151–165.

Aliyu, M.D., Chen, H., Harireche, O., 2016. Finite element modelling for productivity of geothermal reservoirs via extraction well. In: Proceedings of the 24th UK Conference of the Association for Computational Mechanics in Engineering 31 March– 01 April 2016, Cardiff University, Cardiff. Cardiff, pp. 331–334.

Aliyu, M.D., Chen, H., Harireche, O., Hills, C.D., 2017. Numerical Modelling of Geothermal Reservoirs with Multiple Pore Media. In: PROCEEDINGS, 42nd Workshop on Geothermal Reservoir Engineering Stanford University, Stanford, California, February 13-15, 2017 SGP-TR-212. Stanford, US, pp. 1–12.

Bandis, S.C., Lumsden, A.C., Barton, N.R., 1983. Fundamentals of rock joint deformation. Int. J. Rock Mech. Min. Sci. 20, 249–268.

Barton, N., Bandis, S., Bakhtar, K., 1985. Strength, deformation and conductivity coupling of rock joints. Int. J. Rock Mech. Min. Sci. 22, 121–140.

Bažant, Z.P., Ohtsubo, H., 1978. Geothermal heat extraction by water circulation through a large crack in dry hot rock mass. Int. J. Numer. Anal. Methods Geomech. 2, 317–327.

Bažant, Z.P., Ohtsubo, H., Aoh, K., 1979. Stability and post-critical growth of a system of cooling or shrinkage cracks. Int. J. Fract. 15, 443–456.

Dash, Z.V., Murphy, H.D., Aamodt, R.L., Aguilar, R.G., Brown, D.W., Counce, D.A., Fisher, H.N., Grigsby, C.O., Keppler, H., Laughlin, A.W., Potter, R.M., Tester, J.W., Trujillo, P.E., Zyvoloski, G., 1983. Hot dry rock geothermal reservoir testing: 1978 to 1980. J. Volcanol. Geotherm. Res. 15, 59–99.

DuTeaux, R., Swenson, D., Hardeman, B., 1996. Insight from modelling discrete fractures using GEOCRACK. In: 21st Workshop on Geothermal Reservoir Engineering. California, pp. 287–293.

Ghassemi, A., Tarasovs, S., Cheng, A.H.D., 2003. An integral equation solution for three-dimensional heat extraction from planar fracture in hot dry rock. Int. J. Numer. Anal. Methods Geomech. 27, 989–1004.

Harlow, F.H., Pracht, W.E., 1972. A theoretical study of geothermal energy extraction. J. Geophys. Res. 77, 7038–7048.

Hicks, T.W., Pine, R.J., Willis-Richards, J., Xu, S., Jupe, a. J., Rodrigues, N.E.V., 1996. A hydro-thermo-mechanical numerical model for HDR geothermal reservoir evaluation. Int. J. Rock Mech. Min. Sci. Geomech. Abstr. 33, 499–511.

Kelkar, S., WoldeGabriel, G., Rehfeldt, K., 2016. Lessons learned from the pioneering hot dry rock project at Fenton Hill, USA. Geothermics 63, 5–14.

Kohl, T., Evansi, K.F., Hopkirk, R.J., Rybach, L., 1995. Coupled hydraulic, thermal and mechanical considerations for the simulation of hot dry rock reservoirs. Geothermics 24, 345–359.

McFarland, R.D., 1975. Geothermal Reservoir Models--Crack Plane Model, United States Energy Research and Development Administration Contract W-7405-Eng. 36. New Mexico.

Murphy, H.D., Tester, J.W., Grigsby, C.O., Potter, R.M., 1981. Energy extraction from fractured geothermal reservoirs in low-permeability crystalline rock. J. Geophys. Res. 86, 7145.

Taron, J., Elsworth, D., 2009. Thermal–hydrologic–mechanical–chemical processes in the evolution of engineered geothermal reservoirs. Int. J. Rock Mech. Min. Sci. 46, 855–864.

Taron, J., Elsworth, D., 2010. Coupled mechanical and chemical processes in engineered geothermal reservoirs with dynamic permeability. Int. J. Rock Mech. Min. Sci. 47, 1339–1348.

Taron, J., Elsworth, D., Min, K.-B., 2009. Numerical simulation of thermal-hydrologic-mechanical-chemical processes in deformable, fractured porous media. Int. J. Rock Mech. Min. Sci. 46, 842–854.

Willis-Richards, J., 1995. Assessment of hdr reservoir stimulation and performance using simple stochastic models. Geothermics 24, 385–402.

Willis-Richards, J., Wallroth, T., 1995. Approaches to the modelling of HDR reservoirs: A review. Geothermics 24, 307–332.

ISSN 2703-4275